electronics

MDPI

Article

Performance Analysis of Massive MIMO-OFDM System Incorporated with Various Transforms for Image Communication in 5G Systems

Lavish Kansal [1], Salah Berra [2,*], Mohamed Mounir [3], Rajan Miglani [1], Rui Dinis [4] and Khaled Rabie [5,6]

1 School of Electronics & Electrical Engineering, Lovely Professional University, Phagwara 144411, India; lavish.kansal@lpu.co.in (L.K.); rajanmiglani1028@gmail.com (R.M.)
2 COPELABS, Universidade Lusófona de Humanidades e Tecnologias, Campo Grande 376, 1749-024 Lisboa, Portugal
3 Department of Electronics and Communications Engineering, El Gazeera High Institute for Engineering and Technology, Cairo 11751, Egypt; Eng_mohamedvip@yahoo.com
4 Instituto de Telecomunicações, FCT-UNL, Campus de Caparica, 2825-516 Caparica, Portugal; rdinis@fct.unl.pt
5 Department of Engineering, Manchester Metropolitan University, Manchester M15 6BH, UK; k.rabie@mmu.ac.uk
6 Department of Electrical and Electronic Engineering, University of Johannesburg, P. O. Box 17011 Doornfontein, Johannesburg 2028, South Africa
* Correspondence: salahberra39@gmail.com

Abstract: Modern-day applications of fifth-generation (5G) and sixth-generation (6G) systems require fast, efficient, and robust transmission of multimedia information over wireless communication medium for both mobile and fixed users. The hybrid amalgamation of massive multiple input multiple output (mMIMO) and orthogonal frequency division multiplexing (OFDM) proves to be an impressive methodology for fulfilling the needs of 5G and 6G users. In this paper, the performance of the hybrid combination of massive MIMO and OFDM schemes augmented with fast Fourier transform (FFT), fractional Fourier transform (FrFT) or discrete wavelet transform (DWT) is evaluated to study their potential for reliable image communication. The analysis is carried over the Rayleigh fading channels and M-ary phase-shift keying (M-PSK) modulation schemes. The parameters used in our analysis to assess the outcome of proposed versions of OFDM-mMIMO include signal-to-noise ratio (SNR) vs. peak signal-to-noise ratio (PSNR) and SNR vs. structural similarity index measure (SSIM) at the receiver. Our results indicate that massive MIMO systems incorporating FrFT and DWT can lead to higher PSNR and SSIM values for a given SNR and number of users, when compared with in contrast to FFT-based massive MIMO-OFDM systems under the same conditions.

Keywords: massive MIMO; 5G systems; OFDM; DWT; FrFT; image communication; multimedia communications

Citation: Kansal, L.; Berra, S.; Mounir, M.; Miglani, R.; Dinis, R.; Rabie, K. Performance Analysis of Massive MIMO-OFDM System Incorporated with Various Transforms for Image Communication in 5G Systems. *Electronics* **2022**, *11*, 621. https://doi.org/10.3390/electronics11040621

Academic Editor: Raed A. Abd-Alhameed

Received: 17 January 2022
Accepted: 14 February 2022
Published: 17 February 2022

1. Introduction

In this era, the requirement for systems that can support elevated data rates is becoming increasingly important due to the ever-increasing use of applications that allow multimedia transmission, such as virtual reality (VR), 3D videos, and internet of things (IoT) [1,2]. The current pace of technological advancement in the field of image resolutions mandates urgent upgrade of the existing wireless network infrastructure to meet futuristic needs of high-end multimedia data transmission [3,4]. Looking back into various critical evolution junctions in the wireless communication domain, we find the inclusion of OFDM methodology as an important step towards enhancing the data rate transmission. In fact, OFDM has been widely used by many popular standards such as wireless local-area network (WLAN) (e.g., 802.11 a up to 802.11 ax) [5], digital audio broadcasting (DAB) [6], digital video broadcasting (DVB) [7], wireless wide area network (WWAN) (e.g., 802.16 m) [8], and long-term evolution (LTE) [9,10].

OFDM is essentially a multicarrier modulation (MCM) methodology in which the high data rate stream is bifurcated into lower data rate streams [11]. Each stream requires a bandwidth that is much smaller than the coherence bandwidth of the channel, which in turn makes the information in OFDM inherently immune to frequency selective fading. Additionally, the low complexity of OFDM schemes [12] has ensured that fourth-generation (4G) and fifth-generation (5G) mobile networks will also largely rely on OFDM for providing high-speed data access to the end-users. The LTE wireless systems have been implemented based on OFDM in the 4G, which provide various types of traffic, fair scheduling, and balanced Quality of Service (QoS). LTE offers good QoS delivery for distinct traffic classes. The strategy of QoS balancing scheduling rules in an LTE downlink is suggested to provide high QoS delivery for different traffic classes using MU-MIMO [13].

Recently, many enabling technologies such as massive MIMO [14] have been introduced to support data rates beyond 5G (B5G) and sixth generation (6G) networks [4]. In mMIMO base station (BS) is equipped with a huge number of antennas, much larger than the number of serviced users [15,16]. mMIMO increases network capacity and data throughput by splitting data packets over multiple signal paths as well as allowing simultaneous multiple users by using multi-user MIMO (MU-MIMO). mMIMO is, therefore, an enhanced version of MU-MIMO, with advanced features such as increased spectrum efficacy and simplified signal processing, while MU-MIMO was used in the previous mobile generations due to its advantages over point-to-point MIMO, mMIMO is expected to be used in B5G and 6G due to its advantages over MU-MIMO [17,18].

In mMIMO the base station (BS) dedicates a narrow beam towards the direction of each user. The angular beam can be made further narrower and more concentrated in the direction of each user by elevating the number of antennae in the BS. Increasing the number of antennas in the BS not only enhances the sum rate spectral efficiency per cell but also simplifies the required signal processing at both BS and end-users terminals in comparison with MU-MIMO which is largely attributed to channel hardening. Channel hardening precisely refers to a condition when the number of transmitting antennae is large enough to decimate the randomness in the communication channel. As a result, the channel between users and the BS becomes flat with an almost constant gain and additive white Gaussian noise (AWGN) with minimal impact of fading channels and frequency selective fading [19]. Additionally, channel hardening can simplify channel estimation at the users' terminals (i.e., downlink (DL)), while in uplink (UL) the BS runs the channel estimation with the aid of received pilots from each user relying on channel reciprocity between UL and DL in the time division duplexing (TDD) mode [20]. Due to their ability to deliver enhanced quality of the transmission along with very high throughput, many research works advocating the use of mMIMO with OFDM can be found in the literature [21–23] and therefore mMIMO-OFDM becomes an attractive candidate for B5G and 6G networks [24]. However, to the best of our knowledge, no previous work regarding performance evaluation of the image transmission over mMIMO-OFDM link has been reported till date. The quality of image transmission depends on several factors such as received SNR, modulation technique and its order, and other channel-related parameters which can influence the system performance. The transmitter of mMIMO-OFDM is the same as that of conventional OFDM except that pre-coding and re-ordering of all users are carried out in the frequency domain before performing the inverse fast Fourier transform (IFFT). On the other hand, the receiver side of mMIMO-OFDM is similar to that of conventional OFDM [25]. In this work, the performance of mMIMO-OFDM systems based on FFT, DWT, and FrFT is evaluated by sending and receiving the reference baboon image under different SNR values, modulation orders, and a varying number of end-users. The PSNR and SSIM metrics have also been used in evaluating the quality of image transmission.

The rest of this work is arranged as follows; Section 2 discusses the related works in the literature, while Sections 3 and 4 focus on the technical and mathematical analysis required to explain OFDM and mMIMO, respectively. The results are presented in Section 5 while, Section 6 contains the conclusive remarks.

2. Literature Review

Massive MIMO is being enthusiastically hailed as a critical technique for next generation of wireless communication networks applications such as 5G & 6G. mMIMO is equipped with a large number of antennae at the base station to serve the end-users. mMIMO boasts of improved spectral efficiency and high communication reliability [15,26]. Amongst features, the ability of OFDM systems to comprehensively interoperate with various modulation techniques makes it the first choice for massive MIMO systems [27]. In the current scenario, massive MIMO systems use OFDM primarily to overcome effects of flat fading channel and multipath propagation [28,29]. Owing to its robust character and backed by powerful technologies such as OFDM, massive MIMO is bound to be the most sought-after technology for next-generation multi-media data transfer requirements.

Analysis of available literature reveals various previous works that have investigated image transmission over OFDM communication systems. For instance, authors in [30] evaluated the bit error ratio (BER) performance of different signal mapping techniques (i.e., QPSK, 16-PSK, and 16-QAM) for an OFDM-based image transmission system over the AWGN channel. Similarly, authors in [25] analyzed the BER performance for another set of signal mapping schemes (i.e., BPSK, QPSK, 16-PSK, and 256-PSK). In [31], authors have implemented an OFDM-based image transmission system on software-defined radios (SDR) and compared the BER performance in the case of different signal mapping schemes (i.e, BPSK, QPSK, 16-PSK, and 256-PSK). Further, authors in [32] compared image transmission with audio and text transmission using BER and mean-square error (MSE) as comparison metrics. In the same context, the BER of different signal mapping schemes in an OFDM-based image transmission system are compared in the Rayleigh and Rician fading channels in [33,34], respectively. Furthermore, OFDM based image transmission system for an underwater communication channel has been investigated and proposed in [35]. A comparison between FFT-OFDM and DWT-OFDM-based image transmission systems has been presented in [36]. The impact of channel estimation effect on image transmission using OFDM systems has been explained in [37]. The effect of the different channel equalizer types on multi-carrier code-division multiple access (MC-CDMA) based image transmission system was investigated in [38]. It may be further noted here that MC-CDMA is just another version of OFDM in which complex symbols spread throughout all subcarriers in the frequency domain before undergoing IFFT.

Another set of research works has been concerned with managing and reducing a chronic issue in OFDM systems: the Peak to Average Power Ratio (PAPR). For instance, the BER assessment of OFDM based image transmission system after using the companding technique for PAPR reduction has been elaborated in [39,40]. Similarly, [41] evaluated the effect tone reservation (TR) technique for PAPR reduction on the BER assessment of OFDM-based image transmission systems. The effect of reducing the PAPR by using discrete cosine transform (DCT) and DFT precoding techniques on the BER assessment of MC-CDMA-based image transmission system was studied in [42]. In [43], the authors studied the effect of PAPR reduction in visible light communication (VLC) on the BER assessment of OFDM-based image transmission system. The effect of different decoding algorithms on the BER assessment of MIMO-OFDM-based image transmission system has been proposed in [44,45]. The authors of [3] studied the impact of using combining techniques along with diversity order on the BER of different modulation schemes used for image transmission in MIMO-OFDM systems. In [46,47], the authors studied the effect of PAPR reduction on BER, MSE, and PSNR of MIMO-OFDM based image transmission system. Finally, the authors of [48] compared FFT and DCT based MIMO-OFDM image communication systems from SSIM, PSNR, and BER points of view. Pros and cons of previous works have been compared in Table 1. In contrast to the previous works, this work combines mMIMO with OFDM and examines the prposed system performance using pictorial demonstration in addition to PSNR and SSIM. Furthermore, this work investigate the effect of modulation order, number of users, and OFDM transformer type on the performance of the proposed system.

Table 1. Comparison of our work with the previous works.

Ref.	Year	Main Focus of Previous Works	Limitation of Previous Works	Features of Our Study
[30]	2017	Image transmission through OFDM System under the Influence of AWGN channel.	-Study image transmission using single antenna only. -Study image transmission in AWGN only. -Study not includes PSNR and SSIM.	-Study image transmission using massive MIMO combined with OFDM. -Study image transmission in Rayleigh channel. -Study image transmission using various transformers for OFDM. -Study includes effect of number of users. -Study includes PSNR and SSIM.
[25]	2021	Performance evaluation of Image transmission through OFDM system using different PSK schemes under AWGN channel.	-Study image transmission using single antenna only. -Study image transmission in AWGN only. -Study not includes PSNR and SSIM.	-Study image transmission using massive MIMO combined with OFDM. -Study image transmission in Rayleigh channel. -Study image transmission using various transformers for OFDM. -Study includes effect of number of users. -Study includes PSNR and SSIM.
[31]	2020	Implementation of Image transmission system based OFDM using SDR for different PSK schemes.	-Implementation of Image transmission system using single antenna only. -Study not includes PSNR and SSIM.	-Study image transmission using massive MIMO combined with OFDM. -Study image transmission in Rayleigh channel. -Study image transmission using various transformers for OFDM. -Study includes effect number of users. -Study includes PSNR and SSIM.
[32]	2020	Study MSE and BER of Image transmission system based OFDM using different PSK schemes under AWGN channel.	-Study image transmission using single antenna only. -Study image transmission in AWGN only. -Study not includes PSNR and SSIM. -Study not includes pictorial demonstration.	-Study image transmission using massive MIMO combined with OFDM. -Study image transmission in Rayleigh channel. -Study image transmission using various transformers for OFDM. -Study includes effect of number of users. -Study includes pictorial demonstration. -Study includes PSNR and SSIM.
[33]	2017	Image transmission through OFDM System under the Influence of Rayleigh channel.	-Study image transmission using single antenna only. -Study not includes PSNR and SSIM.	-Study image transmission using massive MIMO combined with OFDM. -Study image transmission using various transformers for OFDM. -Study includes effect number of users. -Study includes PSNR and SSIM.
[34]	2019	Image transmission through OFDM System under the Influence of AWGN, Rayleigh, and Rician channels.	-Study image transmission using single antenna only. -Study not includes pictorial demonstration. -Study not includes PSNR and SSIM.	-Study image transmission using massive MIMO combined with OFDM. -Study image transmission using various transformers for OFDM. -Study includes effect of number of users. -Study includes pictorial demonstration. -Study includes PSNR and SSIM.
[35]	2018	Image transmission through OFDM System over underwater fading channels	-Study image transmission using single antenna only. -Study not includes effect of modulation order. -Study not includes SSIM.	-Study image transmission using massive MIMO combined with OFDM. -Study image transmission using various transformers for OFDM. -Study includes effect of modulation order, number of users, and SNR. -Study includes PSNR and SSIM.

Table 1. *Cont.*

Ref.	Year	Main Focus of Previous Works	Limitation of Previous Works	Features of Our Study
[36]	2017	Image transmission through OFDM System based FFT and DWT under the Influence of Rayleigh channel.	-Study image transmission using single antenna only. -Study not includes effect of modulation order. -Study not includes pictorial demonstration. -Study not includes PSNR and SSIM.	-Study image transmission using massive MIMO combined with OFDM. -Study image transmission using various transformers for OFDM. -Study includes effect of modulation order, number of users, and SNR. -Study includes pictorial demonstration. -Study includes PSNR and SSIM.
[37]	2020	Study the effect of channel estimation on the performance of Image transmission system based OFDM under AWGN channel.	-Study image transmission using single antenna only. -Study image transmission in AWGN only. -Study not includes PSNR and SSIM.	-Study image transmission using massive MIMO combined with OFDM. -Study image transmission in Rayleigh channel. -Study image transmission using various transformers for OFDM. -Study includes effect of number of users. -Study includes PSNR and SSIM.
[38]	2019	Study the effect of channel equalization on the performance of Image transmission system based MC-CDMA.	-Study image transmission using single antenna only. -Study not includes effect of modulation order. -Study not includes SSIM.	-Study image transmission using massive MIMO combined with OFDM. -Study image transmission using various transformers for OFDM. -Study includes effect of number of users. -Study includes SSIM.
[39]	2020	Study the effect of PAPR reduction using companding techniques on the performance of Image transmission system based OFDM under AWGN channel.	-Study image transmission using single antenna only. -Study not includes effect of modulation order. -Study image transmission in AWGN only. -Study not includes PSNR and SSIM.	-Study image transmission using massive MIMO combined with OFDM. -Study image transmission in Rayleigh channel. -Study image transmission using various transformers for OFDM. -Study includes effect of modulation order, number of users, and SNR. -Study includes pictorial demonstration. -Study includes PSNR and SSIM.
[41]	2021	Study the effect of PAPR reduction using TR technique on the performance of Image transmission system based OFDM under AWGN channel.	-Study image transmission using single antenna only. -Study not includes effect of modulation order. -Study image transmission in AWGN only. -Study not includes SSIM.	-Study image transmission using massive MIMO combined with OFDM. -Study image transmission in Rayleigh channel. -Study image transmission using various transformers for OFDM. -Study includes effect of modulation order, number of users, and SNR. -Study includes SSIM.
[42]	2019	Study the effect of PAPR reduction using precoding techniques on the performance of Image transmission system based MC-CDMA.	-Study image transmission using single antenna only. -Study not includes effect of modulation order. -Study not includes SSIM.	-Study image transmission using massive MIMO combined with OFDM. -Study image transmission using various transformers for OFDM. -Study includes effect of modulation order, number of users, and SNR. -Study includes SSIM.
[43]	2019	Study the effect of PAPR reduction using precoding on the performance of VLC Image transmission system based OFDM.	-Study image transmission using single antenna only. -Study not includes effect of modulation order. -Study not includes PSNR and SSIM.	-Study image transmission using massive MIMO combined with OFDM. -Study image transmission using various transformers for OFDM. -Study includes effect of modulation order, number of users, and SNR. -Study includes PSNR and SSIM.

Table 1. *Cont.*

Ref.	Year	Main Focus of Previous Works	Limitation of Previous Works	Features of Our Study
[44]	2018	Study the performance of Turbo coding on the performance of Image transmission system based MIMO-OFDM.	-Study image transmission using SU-MIMO only. -Study not includes effect of modulation order. -Study not includes pictorial demonstration. -Study not includes PSNR and SSIM.	-Study image transmission using massive MIMO combined with OFDM. -Study image transmission using various transformers for OFDM. -Study includes effect of number of users, and SNR. -Study includes pictorial demonstration. -Study includes PSNR and SSIM.
[3]	2021	Study the effect of combining techniques on the performance of Image transmission system based MIMO-OFDM.	-Study image transmission using SU-MIMO only. -Study not includes PSNR and SSIM.	-Study image transmission using massive MIMO combined with OFDM. -Study image transmission using various transformers for OFDM. -Study includes effect of number of users. -Study includes PSNR and SSIM.
[46]	2019	Study the effect of PAPR reduction on the performance of Image transmission system based MIMO-OFDM.	-Study image transmission using SU-MIMO only. -Study not includes effect of modulation order. -Study not includes pictorial demonstration. -Study not includes SSIM.	-Study image transmission using massive MIMO combined with OFDM. -Study image transmission using various transformers for OFDM. -Study includes effect of modulation order, number of users, and SNR. -Study includes pictorial demonstration. -Study includes SSIM.
[47]	2019	Study the effect of channel coding on the performance of Image transmission system based MIMO-OFDM under the Influence of AWGN, Rayleigh, and Rician channels.	-Study image transmission using SU-MIMO only. -Study not includes effect of modulation order. -Study not includes SSIM.	-Study image transmission using massive MIMO combined with OFDM. -Study image transmission using various transformers for OFDM. -Study includes effect of modulation order, number of users, and SNR. -Study includes SSIM.
[48]	2020	Study the effect of number of antennas and transformers effect coding on the performance of Image transmission system based MIMO-OFDM under the Influence of AWGN and Rayleigh channels.	-Study image transmission using SU-MIMO only.	-Study image transmission using massive MIMO combined with OFDM. -Study image transmission using various transformers for OFDM. -Study includes effect of number of users.

The key aspects, objectives, and intended outcomes of our proposed research work which derives its inspiration from the literature review presented in this section, can be broadly summed up as:

1. Analysis and evaluation of the possibility of using FRFT and DWT transforms based OFDM multi-user massive MIMO environment instead of conventional FFT transform-based OFDM system for achieving efficient transmission of images.
2. Designing a very efficient and reliable alternative to conventional OFDM system in the form of a hybrid combination of multi-user mMIMO-OFDM system for mobile wireless communication systems.
3. Investigating the performance of the proposed model for a diverse number of users and higher-order modulation schemes.

The implementation of these objectives has been reported in the subsequent sections of this paper.

3. OFDM Methodology

It is used for high data rate transmission over the communication system, where it also solves the problem of multipath and delay time for wireless communication. OFDM uses the multi-carrier to enhance the bandwidth efficiency and data rate [49]. In this work, we use OFDM under the different methods of implementation in FFT, DWT and FrFT. An OFDM transmitter and receiver can be described using the Inverse Discrete Fourier Transform (IDFT) and Discrete Fourier Transform (DFT) blocks [50] and also the IFFT and FFT algorithms are then used to dramatically reduce the system's complexity [51,52]. The transmitted signal data from the user represented as N point of IFFT:

$$x_i = \frac{1}{N}\sum_{n=0}^{N-1} X_n e^{\frac{j2\pi ni}{N}}, \tag{1}$$

and FFT can be represent as:

$$X_n = \frac{1}{N}\sum_{i=0}^{N-1} x_i e^{\frac{-j2\pi ni}{N}}. \tag{2}$$

3.1. DWT Method

The DWT [53] uses the multi-resolution mechanism to simultaneously represent its signal in both frequency and time domain. Wavelet-based systems use a quadrature mirror filter (QMF) bank, which includes a half-band low pass filter (LPF) with an impulse response and a half-band high pass filter (HPF) with an impulse response that convolves with the signal. In OFDM, the FFT can be replaced by DWT to represent the subcarrier as a multi-resolution signal under low and high filter configurations. The transmission data based on DWT can be represented as:

$$x_{j,d} = 2^{\frac{-j}{2}} \sum_{d=-\infty}^{\infty} x_n \Psi(2^{-j}n - d), \tag{3}$$

where d is the shift parameter and Ψ is the mother wavelet, which is constructed in such a way that it may be inverted and the original signal recovered. Then, the IDWT can also present as:

$$x_n = \sum_{d=0}^{\infty}\sum_{j=-\infty}^{\infty} x_{j,d}\Psi(2^{-j}n - d), \tag{4}$$

3.2. FrFT Method

The FrFT can also replace the FFT in the traditional OFDM system, the resulting system methodology is known as FrFT based OFDM system and mathematically it can be represented as:

$$x_n = \sum_{n=0}^{N-1} X_n F_\alpha(m,n), 0 \leqslant m < N, \tag{5}$$

where X_n is the signal data transmitter and $F_\alpha(m,n)$ is the IFrFT transform as detailed explained in [54] , where it can be represented as:

$$F_\alpha(m,n) = \sqrt{\frac{\sin(\alpha) - j.\cos(\alpha)}{N}} \exp(\frac{j}{2}m^2\cot(\alpha(u)^2)\exp(\frac{j}{2}n^2\cot(\alpha))\times \exp(-j\frac{2\pi mn}{N}), \tag{6}$$

where $\alpha = p.\frac{\pi}{2}(0 < \alpha < \pi$, p is the fractional of the transform, u is the sample space. When $\alpha \leq \frac{\pi}{2}$ the transform will be a conventional OFDM.

4. Massive MIMO System Model

Consider a massive MIMO system in Figure 1, where the base station BS is equipped with a large number of antenna M to server single-antenna users K with some time and band frequencies [20]. The receiver baseband signal is given by

$$\mathbf{y} = \sqrt{\mathcal{P}}\mathbf{H}\mathbf{x} + \mathbf{z}, \tag{7}$$

where $\sqrt{\mathcal{P}}x$ is the signal data (where the average of the transmitted power is $\mathcal{P}$), $\mathbf{H}$ is the channel between the BS and the K users which represent the Rayleigh fading channel model and $\mathbf{z}$ is the independent and identical distributed (i.i.d.) AWGN with zero mean and variance $(0, \sigma^2)$ [55]. At the uplink, the linear detection is used to separate K user by multiplying the $M \times K$ weight linear detector matrix A as:

$$\mathbf{y} = \sqrt{\mathcal{P}}\mathbf{A}^H\mathbf{H}\mathbf{x} + \mathbf{A}^H\mathbf{z}, \tag{8}$$

Then, the corresponded elements of kth vector of user, it can be addressed as a receiver signal detection vector as:

$$\mathbf{y}_k = \sqrt{\mathcal{P}}\mathbf{a}^H\mathbf{h}_k\mathbf{x}_k + \sqrt{\mathcal{P}}\sum_{l\neq k}\mathbf{a}^H\mathbf{h}_l\mathbf{x}_l + \mathbf{a}^H\mathbf{z}. \tag{9}$$

Considering the ergodic channel fading, the kth UE's possible uplink SE, $\mathbf{R}_k$, is given by:

$$\mathbf{R}_k = \mathbb{E}\{log_2(1 + \frac{\mathcal{P}|\mathbf{a}^H\mathbf{h}_k\mathbf{x}_k|^2}{\mathcal{P}|\sum_{l\neq k}\mathbf{a}^H\mathbf{h}_l\mathbf{x}_l|^2 + |\mathbf{a}^H\mathbf{z}|^2})\}. \tag{10}$$

Furthermore, the sum of uplink rate can be defined as

$$\mathbf{R} = \sum_{k=1}^{K}\mathbf{R}_k. \tag{11}$$

The weight matrix of linear detection can be conduct with different linear receivers such as MRC, ZF, and MMSE.

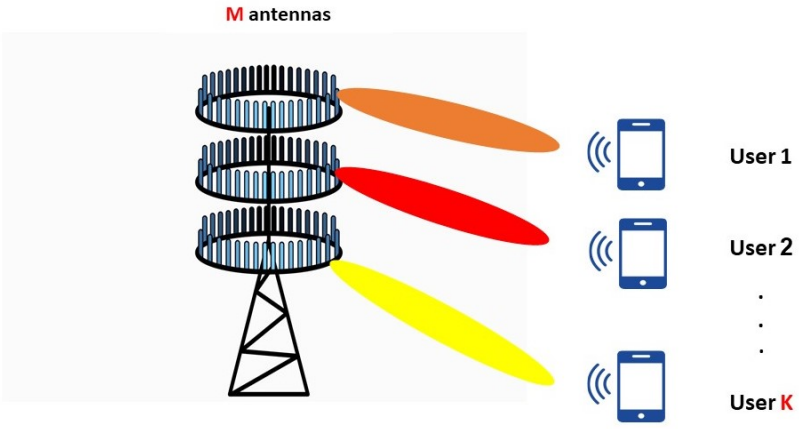

Figure 1. An uplink massive MIMO system.

OFDM-Massive MIMO

Combining the OFDM into massive MIMO as shown in Figure 2. Each user transmits their data into an IFFT-N points block in the uplink, which inserts a cyclic prefix (CP) to the data block before sending it through the channel. CP is a component of the block's end that is added to the block's beginning. The received signal of each BS antenna is sent via an FFT-N points block at the BS after the CP is removed, and the resulting signals are given to the detection methods such as zero forcing or minim square error MMSE. Figure 3 represents

the flowchart for the proposed OFDM Massive MIMO system to achieve a desired PSNR and SSIM values. The transmitted signal data from each user is represented as N point of IFFT [56]

$$\mathbf{x}_{k,i} = \frac{1}{N} \sum_{k=1}^{K} \sum_{n=0}^{N-1} \mathbf{X}_{k,n} e^{\frac{j2\pi ni}{N}}, \tag{12}$$

where $\mathbf{x}_{k,i}$ is the i-th component of the vector transmitted from the k-th antenna. After adding CP the frequency domain representation of the received signal can be expressed as:

$$\begin{aligned} \hat{\mathbf{x}}_{m,i} &= \frac{1}{N} \sum_{m=0}^{M-1} \sum_{k=1}^{K} \sum_{n=0}^{N-1} \mathbf{Y}_{k,m,n} e^{\frac{j2\pi ni}{N}} \\ &= \frac{1}{N} \sum_{q=0}^{N-1} \sum_{m=0}^{M-1} \sum_{k=1}^{K} \sum_{n=0}^{N-1} \mathbf{H}_{k,m,n} \mathbf{x}_{m,q} e^{\frac{j2\pi n(i-q)}{N}} + \eta_{m,i}, \end{aligned} \tag{13}$$

where $\eta_{m,i}$ is the i-th element of the zero-mean complex white Gaussian noise with variance added to the m-th antenna of BS. Implementing OFDM-DWT with massive MIMO system can be addressed. The signal transmission from each user K is defined as:

$$\mathbf{x}_{k,n} = \sum_{k=1}^{K} \sum_{d=0}^{\infty} \sum_{j=-\infty}^{\infty} \mathbf{X}_{k,j,d} \Psi(2^{-j} n - d). \tag{14}$$

After the signal passes through the channel and receiver, the resulting receiver signal can be represented as:

$$\hat{\mathbf{X}}_{m,j,d} = \sum_{k=1}^{K} \sum_{d=0}^{\infty} \sum_{j=-\infty}^{\infty} \mathbf{x}_{k,m,j,d} \Psi(2^{-j} n - d) \mathbf{H}_{k,m,j,d} + \eta_{m,i,d}. \tag{15}$$

On replacing FFT with FrFT, the receiver signal can be mathematically written as:

$$\hat{\mathbf{X}}_{m,j,d} = \sum_{k=1}^{K} \sum_{d=0}^{\infty} \sum_{j=-\infty}^{\infty} \mathbf{x}_{k,m,j,d} F_{\alpha}(m,n) \mathbf{H}_{k,m,j,d} + \eta_{m,i,d}. \tag{16}$$

All of the above equations represent the OFDM with different design methods such as FFT, DWT and Frft, with different parameters.

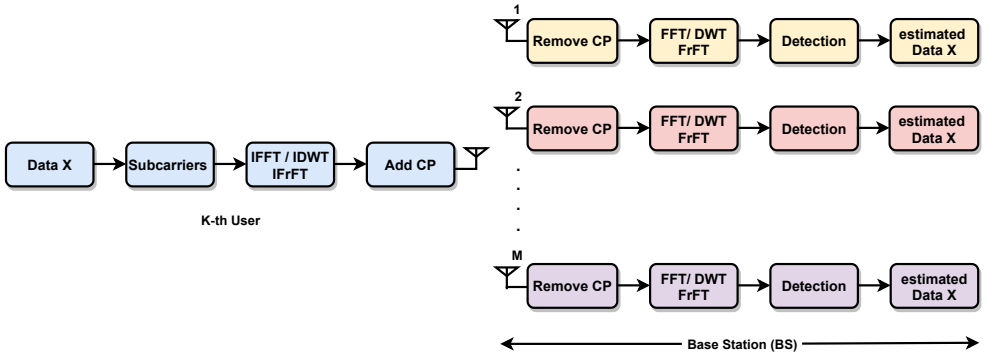

Figure 2. Block diagram of OFDM Massive MIMO systems in the uplink.

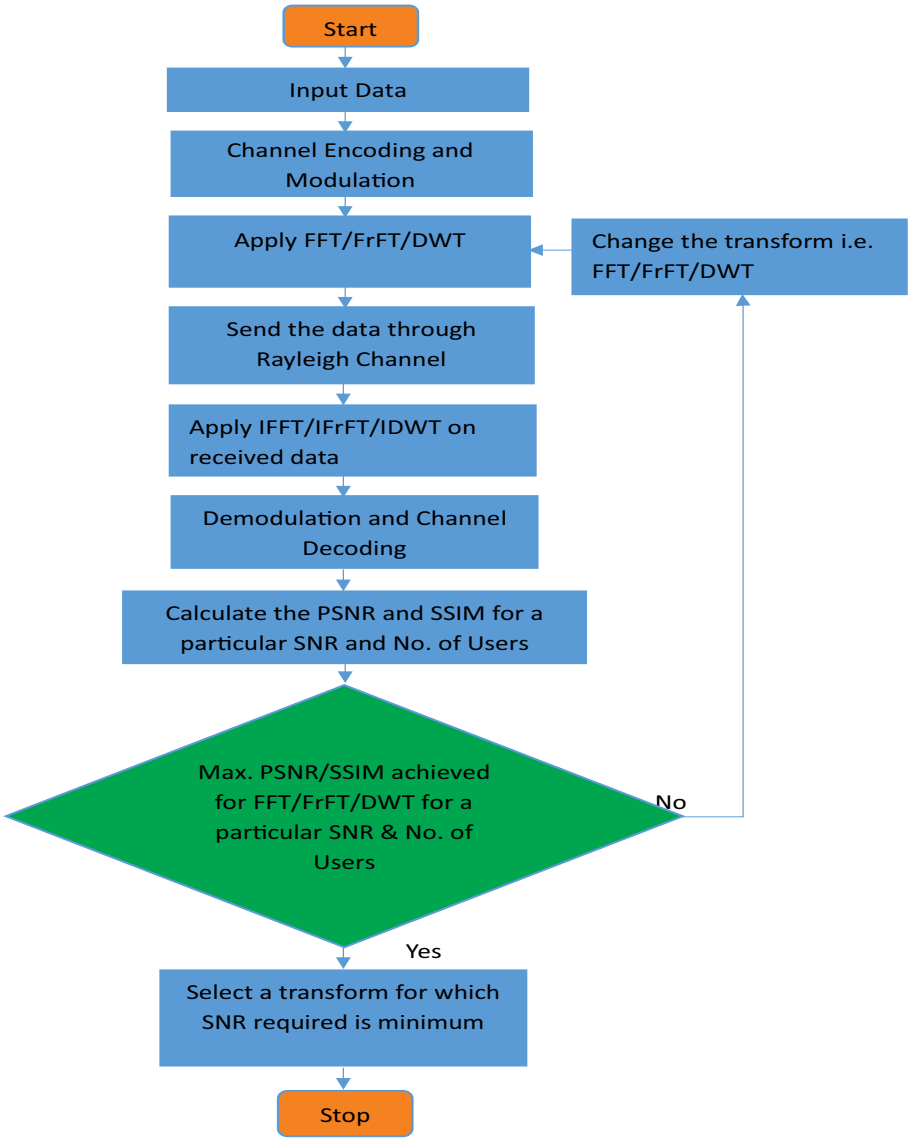

Figure 3. A flowchart of the proposed OFDM Massive MIMO systems.

5. Performance Results

The performance assessment of Massive MIMO incorporated by FFT-OFDM, FRFT-OFDM, and DWT-OFDM multi-carrier modulation scheme is presented for image transmission. In Figures 4–21, a pictorial demonstration of image excellence is depicted for FFT-OFDM, FRFT-OFDM, and DWT-OFDM with varying number of users, different modulation levels, and different SNR values. Simulation parameters are given in Table 2.

It is very clear from Figures 4–21 that for any implementation method (i.e., FFT, FRFT, or DWT) and any modulation order, increasing SNR value from 10 d to 30 dB (i.e., column-wise) improves the received image quality, for the same number of users. On the other hand, an increasing number of users from 10 to 50 (i.e., row-wise) degrades the received signal quality for the same SNR value.

Moreover, it can be noted that as the modulation order is increased, the received image quality keeps on deteriorating for a given particular SNR value and number of users, regardless of the implementation method. Clearly, in the case of FFT-OFDM, the received image quality decreases with increasing modulation level from BPSK in Figure 4 to 64-PSK in Figure 9, assuming a certain SNR value and the same number of users. In the case of FRFT-OFDM and DWT-OFDM, the same thing can be seen in Figures 10–21, respectively.

Furthermore, the comparison of Figures 4–21 depict that for any modulation order, e.g., BPSK, the received image quality in case of DWT (i.e., Figure 16) is better than the received image quality in case of FRFT (i.e., Figure 10) and the received image quality in case of FRFT (i.e., Figure 10) is better than the received image quality in case of FFT (i.e., Figure 4). This fact is clearly demonstrated at low SNR values (i.e., SNR = 0 dB and SNR = 10 dB) and a large number of users (i.e., n = 50). However, at high order modulation (i.e., 64-PSK), this fact cannot be demonstrated pictorially; instead, PSNR and SSIM are used to examine the difference in the quality of the received signal, as will be illustrated in Figures 22 and 23. The pictorial demonstration vindicates that fact for a particular modulation level and number of uses, the DWT-OFDM gives the best image quality at a particular SNR level.

Figures 22 and 23 illustrates the variations of the PSNR and SSIM with SNR for Massive MIMO incorporated by FFT-OFDM, FRFT-OFDM, and DWT-OFDM over Rayleigh channel for the different number of users. It is clear from the observations of Figure 22 that there is a substantial degradation in the PSNR values for FFT-OFDM, FRFT-OFDM and DWT-OFDM on increasing the number of users from 10 to 50. In the case of FFT-OFDM employing BPSK at SNR = 10 dB for 10 users, the PSNR value is 21.76 dB, and it is decreased up to 15.45 dB for 20 users, and 13.14 dB when the number of users increases to 50. Similar inferences can be made on careful observation of PSNR variations for FRFT-OFDM and DWT-OFDM for various modulation levels, SNR values, and number of users. However, if we compare the SNR vs. PSNR performance of FFT-OFDM, FRFT-OFDM and DWT-OFDM, it is very evident that the DWT-OFDM performs better in comparison to FFT-OFDM and FRFT-OFDM. In the case of BPSK at SNR = 10 dB, the PSNR value is 21.76 dB, and it increases to 48.43 dB for FRFT-OFDM, however, the PSNR elevates to 52.55 dB for DWT-OFDM. Similar reasoning can be made out from careful observation of PSNR variations for various modulation levels, SNR values, and number of users. This increase in PSNR values results in significant improvement in the quality of the image at the receiver end. Careful observation of Figure 23 reveals that SSIM values keeps on decreasing as the number of users increases from 10 to 50 or the modulation level increases from BPSK to 64-PSK. However, the SSIM values for DWT-OFDM is better than FRFT-OFDM and FFT-OFDM.

Table 2. Simulation Parameters.

Parameter	**Value**
N_{FFT} Number of subcarriers	256
Cyclic Prefix	1/4
Transform	FFT, FrFT, DWT
Convolution Code Rate	1/2
Modulation Type	*M-PSK*
Modulation order	2, 4, 8, 16, 32, 64
Simulated Environment	Rayleigh Channel (NLOS)
Total No. of OFDM Symbols used for Simulation	10^6
Detection technique	minimum mean square error (MMSE)
No. of Users	10, 20, 50

(**a**)

(**b**)

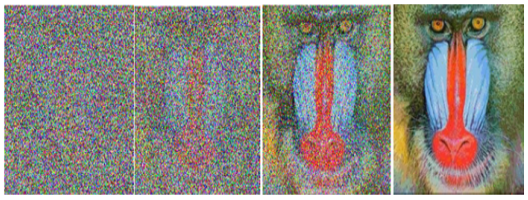

(**c**)

Figure 4. Received Image with Massive MIMO incorporated FFT-OFDM over a Rayleigh channel, Modulated with BPSK and at SNR = 0, 10, 20, 30 dB from Left to Right for different number of users, n. (**a**) n = 10; (**b**) n = 20; (**c**) n = 50.

(**a**)

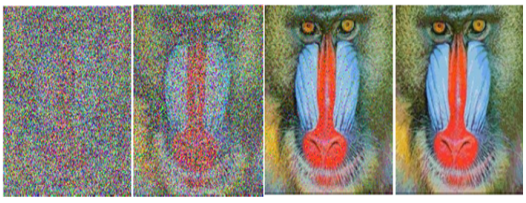

(**b**)

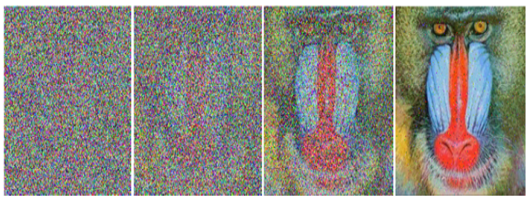

(**c**)

Figure 5. Received image with massive MIMO incorporated FFT-OFDM over a Rayleigh channel, Modulated with QPSK and at SNR = 0, 10, 20, 30 dB from Left to Right for different number of users, n. (**a**) n = 10; (**b**) n = 20; (**c**) n = 50.

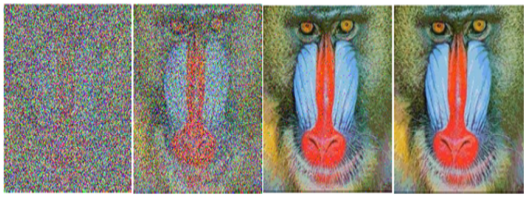

(**a**)

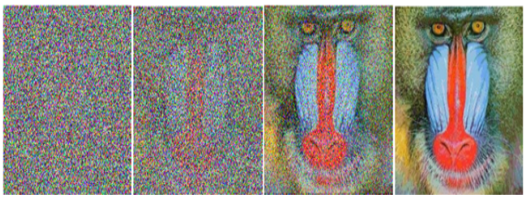

(**b**)

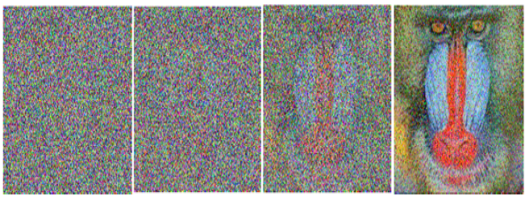

(**c**)

Figure 6. Received image with massive MIMO incorporated FFT-OFDM over a Rayleigh channel, Modulated with 8-PSK and at SNR = 0, 10, 20, 30 dB from Left to Right for different number of users, n. (**a**) n = 10; (**b**) n = 20; (**c**) n = 50.

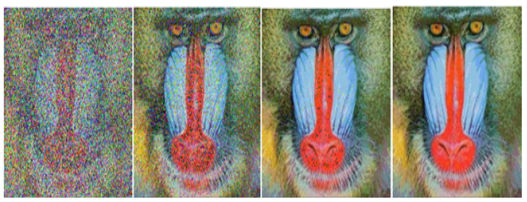

(**a**)

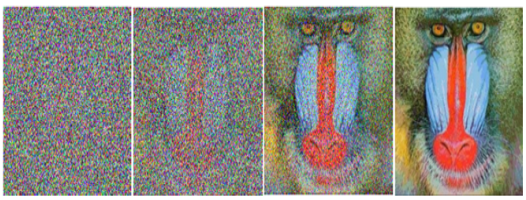

(**b**)

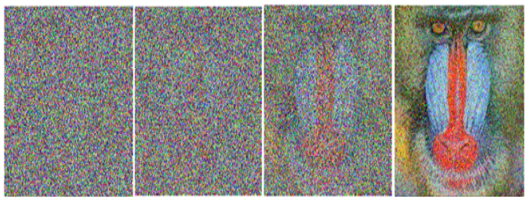

(**c**)

Figure 7. Received image with massive MIMO incorporated FFT-OFDM over a Rayleigh channel, Modulated with 16-PSK and at SNR = 0, 10, 20, 30 dB from Left to Right for different number of users, n. (**a**) n = 10; (**b**) n = 20; (**c**) n = 50.

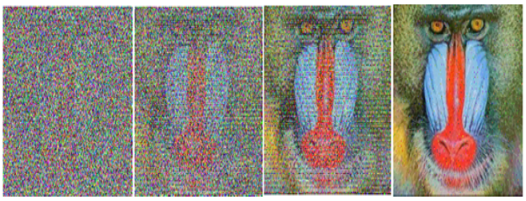

(**a**)

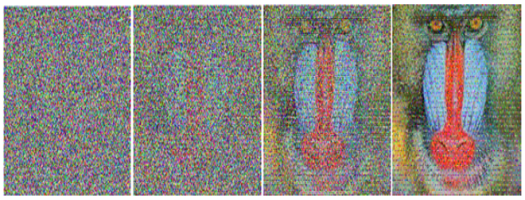

(**b**)

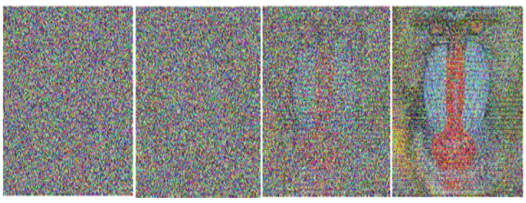

(**c**)

Figure 8. Received image with massive MIMO incorporated FFT-OFDM over a Rayleigh channel, Modulated with 32-PSK and at SNR = 0, 10, 20, 30 dB from Left to Right for different number of users, n. (**a**) n = 10; (**b**) n = 20; (**c**) n = 50.

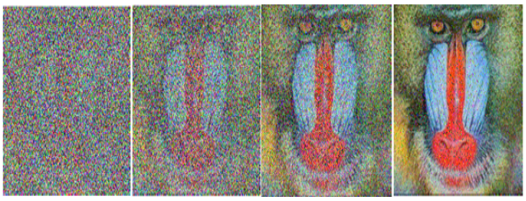

(**a**)

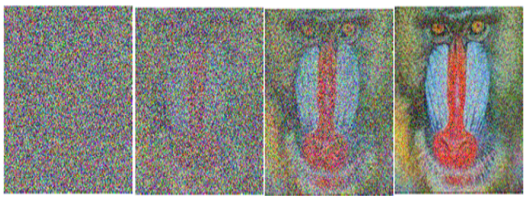

(**b**)

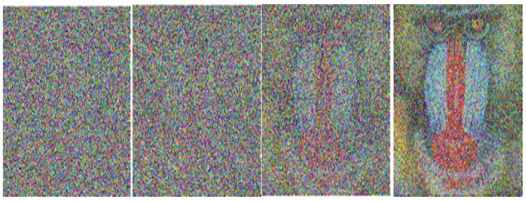

(**c**)

Figure 9. Received image with massive MIMO incorporated FFT-OFDM over a Rayleigh channel, Modulated with 64-PSK and at SNR = 0, 10, 20, 30 dB from Left to Right for different number of users, n. (**a**) n = 10; (**b**) n = 20; (**c**) n = 50.

(**a**)

(**b**)

(**c**)

Figure 10. Received image with massive MIMO incorporated FRFT-OFDM over a Rayleigh channel, Modulated with BPSK and at SNR = 0, 10, 20, 30 dB from Left to Right for different number of users, n. (**a**) n = 10; (**b**) n = 20; (**c**) n = 50.

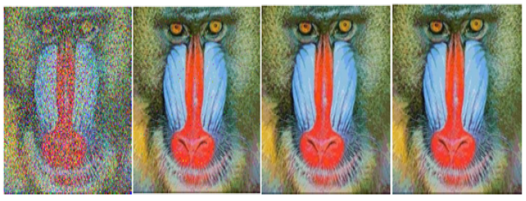

(**a**)

(**b**)

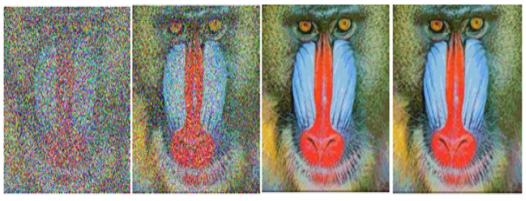

(**c**)

Figure 11. Received image with massive MIMO incorporated FRFT-OFDM over a Rayleigh channel, Modulated with QPSK and at SNR = 0, 10, 20, 30 dB from Left to Right for different number of users, n. (**a**) n = 10; (**b**) n = 20; (**c**) n = 50.

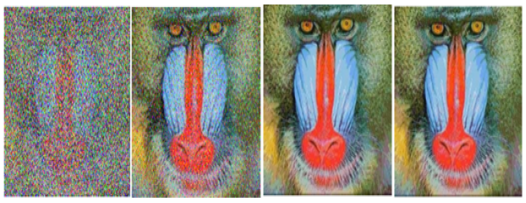

(**a**)

(**b**)

(**c**)

Figure 12. Received image with massive MIMO incorporated FRFT-OFDM over a Rayleigh channel, Modulated with 8-PSK and at SNR = 0, 10, 20, 30 dB from Left to Right for different number of users, n. (**a**) n = 10; (**b**) n = 20; (**c**) n = 50.

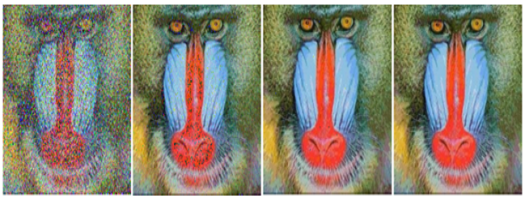

(**a**)

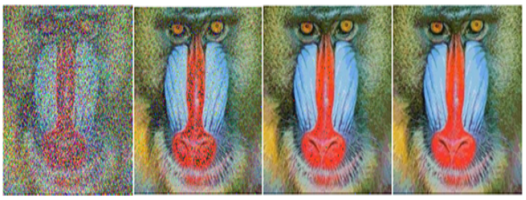

(**b**)

(**c**)

Figure 13. Received image with massive MIMO incorporated FRFT-OFDM over a Rayleigh channel, Modulated with 16-PSK and at SNR = 0, 10, 20, 30 dB from Left to Right for different number of users, n. (**a**) n = 10; (**b**) n = 20; (**c**) n = 50.

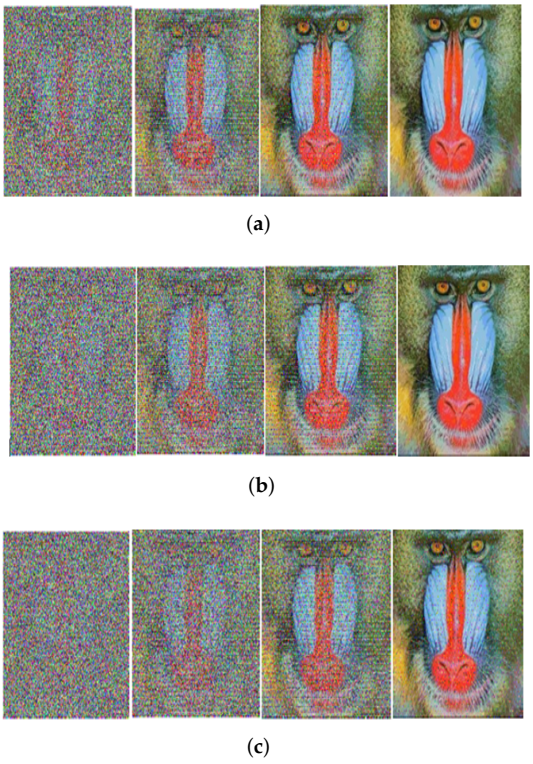

(**a**)

(**b**)

(**c**)

Figure 14. Received image with massive MIMO incorporated FRFT-OFDM over a Rayleigh channel, Modulated with 32-PSK and at SNR = 0, 10, 20, 30 dB from Left to Right for different number of users, n. (**a**) n = 10; (**b**) n = 20; (**c**) n = 50.

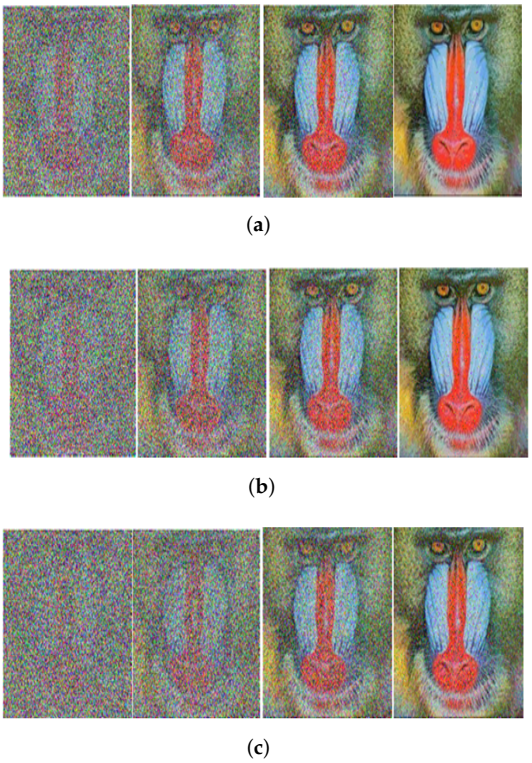

(**a**)

(**b**)

(**c**)

Figure 15. Received image with massive MIMO incorporated FRFT-OFDM over a Rayleigh channel, Modulated with 64-PSK and at SNR = 0, 10, 20, 30 dB from Left to Right for different number of users, n. (**a**) n = 10; (**b**) n = 20; (**c**) n = 50.

(**a**)

(**b**)

(**c**)

Figure 16. Received image with massive MIMO incorporated DWT-OFDM over a Rayleigh channel, Modulated with BPSK and at SNR = 0, 10, 20, 30 dB from Left to Right for different number of users, n. (**a**) n = 10; (**b**) n = 20; (**c**) n = 50.

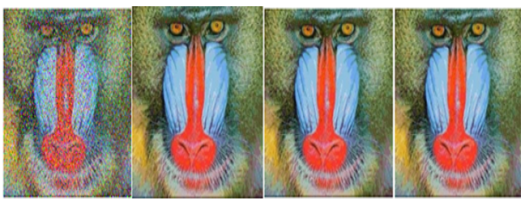

(**a**)

(**b**)

(**c**)

Figure 17. Received image with massive MIMO incorporated DWT-OFDM over a Rayleigh channel, Modulated with QPSK and at SNR = 0, 10, 20, 30 dB from Left to Right for different number of users, n. (**a**) n = 10; (**b**) n = 20; (**c**) n = 50.

(**a**)

(**b**)

(**c**)

Figure 18. Received image with massive MIMO incorporated DWT-OFDM over a Rayleigh channel, Modulated with 8-PSK and at SNR = 0, 10, 20, 30 dB from Left to Right for different number of users, n. (**a**) n = 10; (**b**) n = 20; (**c**) n = 50.

(**a**)

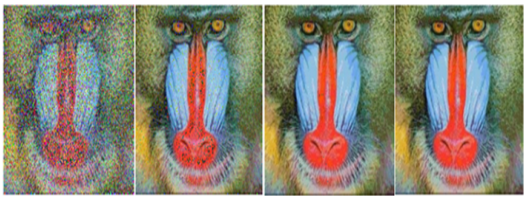

(**b**)

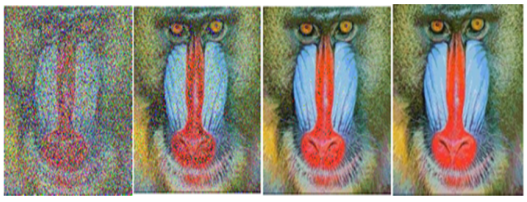

(**c**)

Figure 19. Received image with massive MIMO incorporated DWT-OFDM over a Rayleigh channel, Modulated with 16-PSK and at SNR = 0, 10, 20, 30 dB from Left to Right for different number of users, n. (**a**) n = 10; (**b**) n = 20; (**c**) n = 50.

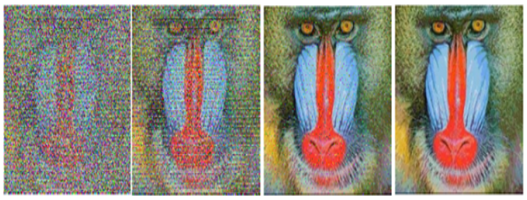

(**a**)

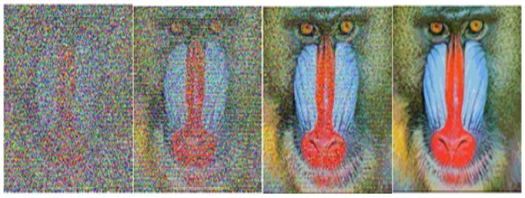

(**b**)

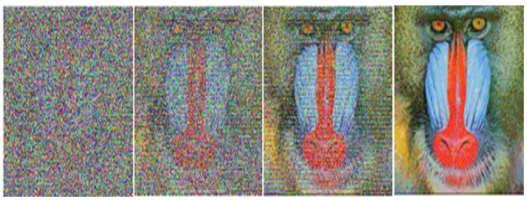

(**c**)

Figure 20. Received image with massive MIMO incorporated DWT-OFDM over a Rayleigh channel, Modulated with 32-PSK and at SNR = 0, 10, 20, 30 dB from Left to Right for different number of users, n. (**a**) n = 10; (**b**) n = 20; (**c**) n = 50.

(**a**)

(**b**)

(**c**)

Figure 21. Received image with massive MIMO incorporated DWT-OFDM over a Rayleigh channel, Modulated with 64-PSK and at SNR = 0, 10, 20, 30 dB from Left to Right for different number of users, n. (**a**) n = 10; (**b**) n = 20; (**c**) n = 50.

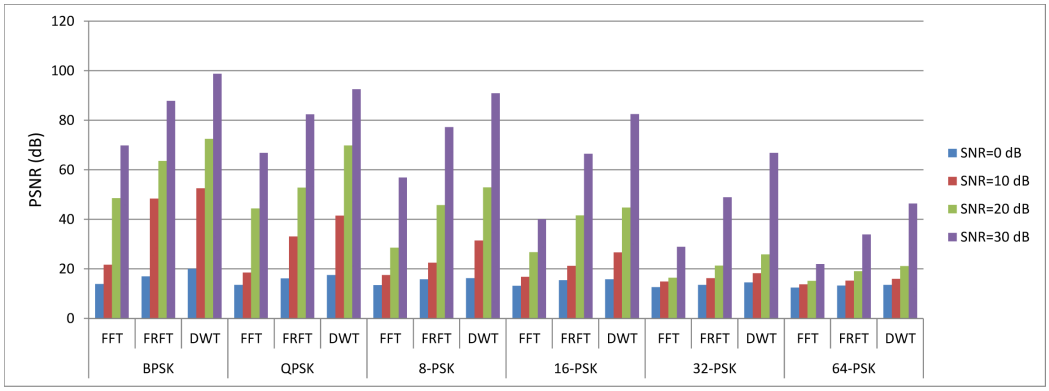

(a)

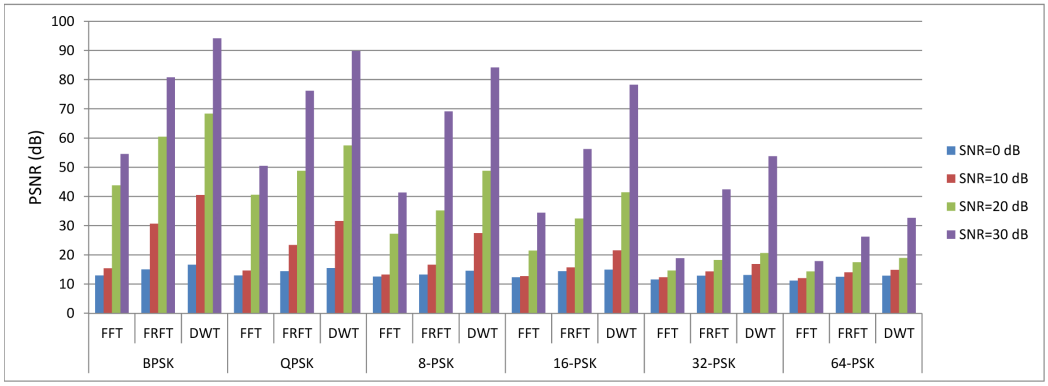

(b)

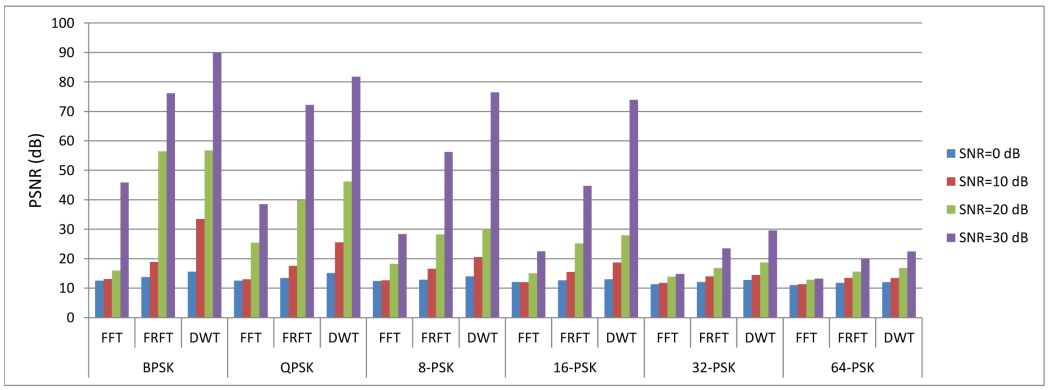

(c)

Figure 22. PSNR variations for Massive MIMO incorporated FFT-OFDM, FRFT-OFDM and DWT-OFDM for various modulation levels and number of users over Rayleigh Channel. (**a**) $n = 10$; (**b**) $n = 20$; (**c**) $n = 50$.

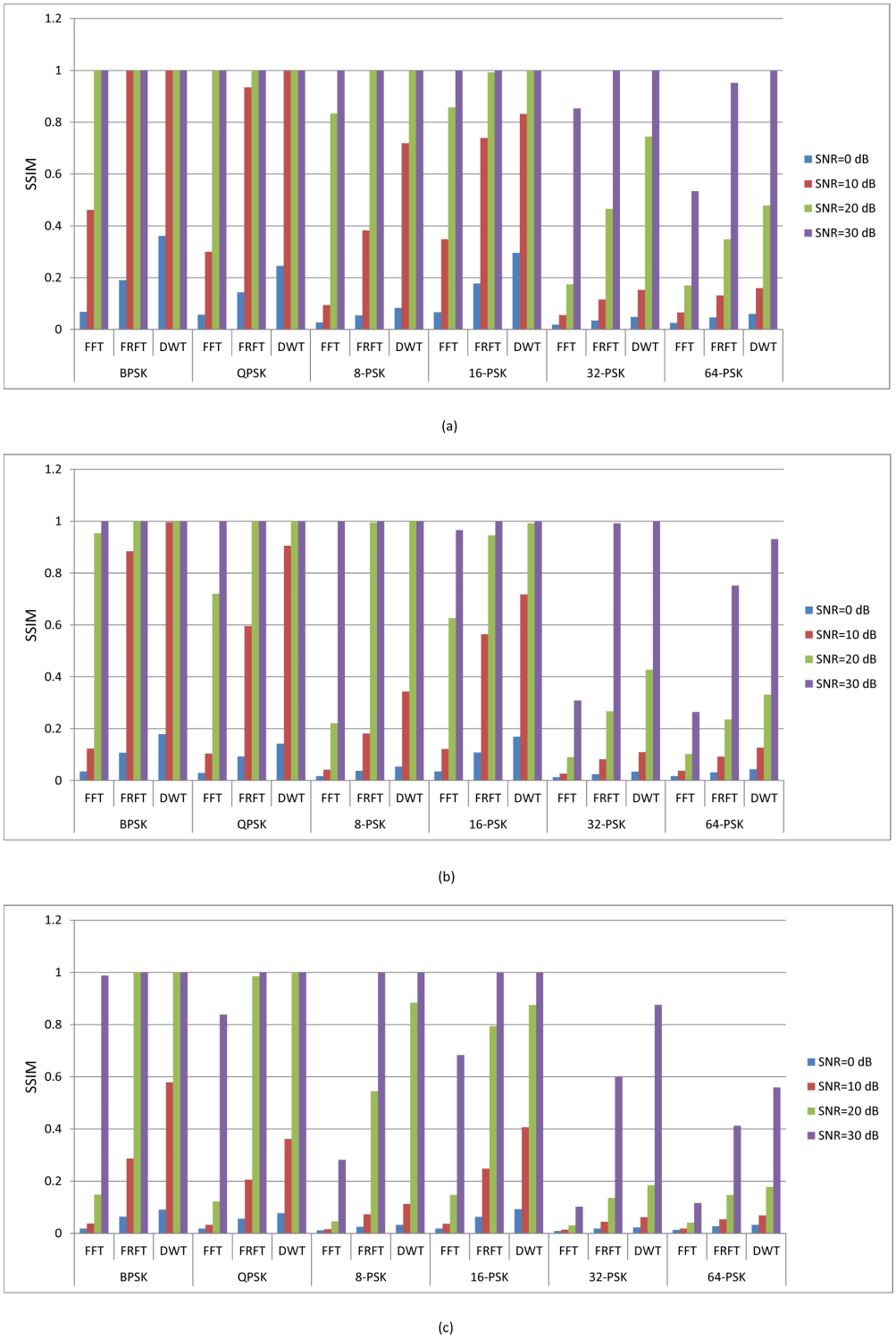

Figure 23. SSIM variations for Massive MIMO incorporated FFT-OFDM, FRFT-OFDM and DWT-OFDM for various modulation levels and number of users over Rayleigh Channel. (**a**) $n = 10$; (**b**) $n = 20$; (**c**) $n = 50$.

6. Conclusions

In this paper, the idea of fast, bandwidth-efficient, and robust image communication required for 5G and 6G systems is presented by using a hybrid combination of massive MIMO and OFDM systems augmented with diverse transforms, i.e., FFT, FrFT and DWT. The analysis is presented for the Rayleigh fading channel for different levels of M-PSK modulation technique. It is very evident from the simulation outcome that the image

quality deteriorates when the number of users increases from 10 to 50 for a given value of SNR. However, if we increase the SNR, we can see an improvement in the received image quality. On comparing the received image quality of hybrid combination of massive MIMO and OFDM augmented with FFT, FrFT and DWT transforms, it is observed that the received image quality in the case of FrFT augmented OFDM is much better than the OFDM system augmented with FFT. However, if we replace the FrFT transform with DWT we can see a significant improvement in the received image quality. In addition to the visual inspection, the image quality enhancement also can be accessed by the reported values of PSNR and SSIM. Our analysis also revealed that the values of PSNR and SSIM for DWT augmented OFDM is better than the FrFT and FFT augmented OFDM. However, if the number of users keeps on increasing, there is a decrease in the PSNR and SSIM values for all the diverse modulation levels and transformation techniques.

In the future, a hybrid combination of massive MIMO, generalized frequency division multiplexing (GFDM) and filter band multi-carrier (FBMC) techniques can be explored to support the multimedia application for 5G/6G users as no cyclic prefix is required in GFDM and FBMC. Additionally, the assessment of hybrid amalgamation of OFDM and massive MIMO can be evaluated for other signal detection techniques such as zero-forcing and mean squared error (MSE).

Author Contributions: Conceptualization, L.K., S.B., M.M.; methodology, S.B., R.M.; software, L.K., S.B.; validation, L.K., S.B. and M.M.; formal analysis, S.B., R.M.; investigation, R.D., K.R. and R.M.; resources, M.M., S.B. and L.K.; data analysis, L.K. and S.B.; writing—original draft preparation, L.K., S.B., M.M. and R.M.; writing—review and editing, R.M., R.D. and K.R.; visualization, R.M., R.D. and K.R.; supervision, R.M.; project administration, R.M. and S.B.; funding acquisition, R.D. All authors have read and agreed to the published version of the manuscript.

Funding: Fundação para a Ciência e Tecnologia.

Data Availability Statement: All data that support the findings of this study are included within the article.

Acknowledgments: This work was supported by FCT/MCTES through national funds and when applicable co-funded EU funds under the project MASSIVE5G (PTDC/EEI-TEL/30588/2017), Copelabs (UIDB/04111/2020), and Instituto de Telecomunicações (UIDB/50008/2020).

Conflicts of Interest: The authors declare no conflict of interest.

Abbreviations

The following abbreviations are used in this manuscript:

4G	Fourth Generation Mobile Networks
5G	Fifth Generation Mobile Networks
6G	Sixth Generation Mobile Networks
AWGN	Additive White Gaussian Noise
B5G	Beyond 5G
BER	Bit Error Rate
BPSK	Binary Phase Shift Keying
BS	Base Station
CP	Cyclic Prefix
DAB	Digital Audio Broadcasting
DCT	Discrete Cosine Transform
DFT	Discrete Fourier Transform

DL	Downlink
DVB	Digital Video Broadcasting
DWT	Discrete Wavelet Transform
FFT	Fast Fourier transform
FRFT	Fractional Fourier Transform
HPF	High Pass Filter
IDFT	Inverse Discrete Fourier Transform
IDWT	Inverse Discrete Wavelet Transform
IFFT	Inverse Fast Fourier Transform
IFRFT	Inverse Fractional Fourier Transform
LPF	Low Pass Filter
MC-CDMA	Multi Carrier Code Division Multiple
MCM	Multicarrier Modulation
MIMO	Multiple Input Multiple Output
mMIMO	Massive Multiple Input Multiple Output
M-PSK	M-ary Phase Shift Keying
MSE	Mean-Square Error
MU-MIMO	Multi-User MIMO
OFDM	Orthogonal Frequency Division Multiplexing
PAPR	Peak to Average Power Ratio
PSNR	Peak Signal-to-Noise Ratio
QAM	Quadrature Amplitude Modulation
QMF	Quadrature Mirror Filter
QPSK	Quadrature Phase Shift Keying
SDR	Software Defined Radios
SNR	Signal-to-Noise Ratio
SSIM	Structural Similarity Index Measure
TDD	Time Division Duplexing
TR	Tone Reservation
UL	Uplink
VLC	Visible Light Communication
WLAN	Wireless Local-Area Network
WWAN	Wireless Wide Area Network

References

1. Hazarika, A.; Poddar, S.; Nasralla, M.M.; Rahaman, H. Area and energy efficient shift and accumulator unit for object detection in IoT applications. *Alex. Eng. J.* **2022**, *61*, 795–809. [CrossRef]
2. Nasralla, M.M.; Hewage, C.; Martini, M.G. Subjective and objective evaluation and packet loss modeling for 3D video transmission over LTE networks. In Proceedings of the 2014 International Conference on Telecommunications and Multimedia (TEMU), Heraklion, Greece, 28–30 July 2014; pp. 254–259. [CrossRef]
3. Sharma, A.; Kansal, L.; Gaba, G.S.; Mounir, M. Image Transmission Analysis Using MIMO-OFDM Systems. In *Enabling Technologies for Next Generation Wireless Communications*; CRC Press: Boca Raton, FL, USA, 2021; pp. 195–209.
4. Imoize, A.L.; Adedeji, O.; Tandiya, N.; Shetty, S. 6G Enabled Smart Infrastructure for Sustainable Society: Opportunities, Challenges, and Research Roadmap. *Sensors* **2021**, *21*, 1709. [CrossRef]
5. *IEEE Standard for Information Technology–Telecommunications and Information Exchange between Systems Local and Metropolitan Area Networks–Specific Requirements Part 11: Wireless LAN Medium Access Control (MAC) and Physical Layer (PHY) Specifications Amendment 1: Enhancements for High-Efficiency WLAN*; IEEE Std 802.11ax-2021 (Amendment to IEEE Std 802.11-2020); IEEE: Piscataway, NJ, USA , 2021; pp. 1–767. [CrossRef]
6. ETSI. *Radio Broadcasting Systems; Digital Audio Broadcasting (DAB) to Mobile, Portable and Fixed Receivers*; ETSI ETS 300 401 (edition 1); ETSI: Sophia Antipolis, France, 2017.
7. Digital Video Broadcasting (DVB). *Second Generation Framing Structure, Channel Coding and Modulation Systems for Broadcasting, Interactive Services, News Gathering and Other Broadband Satellite Applications*; Part 2: DVB-S2 Extensions (DVB-S2X); ETSI EN 302 307-2 V1.3.1; ETSI: Sophia Antipolis, France, 2014 .
8. *IEEE Standard for Air Interface for Broadband Wireless Access Systems*; IEEE Std 802.16-2017 (Revision of IEEE Std 802.16-2012); IEEE: Piscataway, NJ, USA , 2018; pp. 1–2726. [CrossRef]
9. Nasralla, M.M. A Hybrid Downlink Scheduling Approach for Multi-Traffic Classes in LTE Wireless Systems. *IEEE Access* **2020**, *8*, 82173–82186. [CrossRef]

10. Nasralla, M.M.; Khan, N.; Martini, M.G. Content-aware downlink scheduling for LTE wireless systems: A survey and performance comparison of key approaches. *Comput. Commun.* **2018**, *130*, 78–100. [CrossRef]
11. Zerhouni, K.; Amhoud, E.M.; Chafii, M. Filtered Multicarrier Waveforms Classification: A Deep Learning-Based Approach. *IEEE Access* **2021**, *9*, 69426–69438. [CrossRef]
12. Orthogonal Frequency Division Multiplexing (OFDM). In *Digital Communication For Practicing Engineers*; John Wiley & Sons, Ltd.: Hoboken, NJ, USA, 2019; Chapter 10, pp. 453–504. [CrossRef]
13. Nasralla, M.M.; Razaak, M.; Rehman, I.; Martini, M.G. A Comparative Performance Evaluation of the HEVC Standard with its Predecessor H.264/AVC for Medical videos over 4G and beyond Wireless Networks. In Proceedings of the 2018 8th International Conference on Computer Science and Information Technology (CSIT), Amman, Jordan, 11–12 July 2018; pp. 50–54. [CrossRef]
14. Yang, P.; Xiao, Y.; Xiao, M.; Li, S. 6G Wireless Communications: Vision and Potential Techniques. *IEEE Netw.* **2019**, *33*, 70–75. [CrossRef]
15. Berra, S.; Albreem, M.A.; Abed, M.S. A Low Complexity Linear Precoding Method for Massive MIMO. In Proceedings of the 2020 International Conference on UK-China Emerging Technologies (UCET), Glasgow, UK, 20–21 August 2020; pp. 1–4.
16. Berra, S.; Albreem, M.A.M.; Malek, M.; Dinis, R.; Li, X.; Rabie, K.M. A Low-Complexity Soft-Output Signal Data Detection Algorithm for UL Massive MIMO Systems. In Proceedings of the 2021 International Conference on Computer, Information and Telecommunication Systems (CITS), Istanbul, Turkey, 11–13 November 2021; pp. 1–6. [CrossRef]
17. Lu, L.; Li, G.Y.; Swindlehurst, A.L.; Ashikhmin, A.; Zhang, R. An Overview of Massive MIMO: Benefits and Challenges. *IEEE J. Sel. Top. Signal Processing* **2014**, *8*, 742–758. [CrossRef]
18. Salah, I.; Mabrook, M.M.; Rahouma, K.H.; Hussein, A.I. Energy efficiency optimization in adaptive massive MIMO networks for 5G applications using genetic algorithm. *Opt. Quantum Electron.* **2022**, *54*, 125. [CrossRef]
19. Imoize, A.L.; Ibhaze, A.E.; Atayero, A.A.; Kavitha, K. Standard propagation channel models for MIMO communication systems. *Wirel. Commun. Mob. Comput.* **2021**, *2021*, 8838792. [CrossRef]
20. Marzetta, T.L. *Fundamentals of Massive MIMO*; Cambridge University Press: Cambridge, UK, 2016.
21. Subitha, D.; Vani, R. Analysis of Linear Precoding Techniques for Massive MIMO-OFDM Systems under various scenarios. *IOP Conf. Ser. Mater. Sci. Eng.* **2021**, *1084*, 012053. [CrossRef]
22. Zhang, R.; Hao, W.; Sun, G.; Yang, S. Hybrid Precoding Design for Wideband THz Massive MIMO-OFDM Systems With Beam Squint. *IEEE Syst. J.* **2021**, *15*, 3925–3928. [CrossRef]
23. Tu, Y.P.; Chen, C.Y.; Lin, K.H. An Efficient Two-Stage Receiver Base on AOR Iterative Algorithm and Chebyshev Acceleration for Uplink Multiuser Massive-MIMO OFDM Systems. *Electronics* **2022**, *11*, 92. [CrossRef]
24. Riadi, A.; Boulouird, M.; Hassani, M.M. ZF and MMSE detectors performances of a Massive MIMO system combined with OFDM and M-QAM modulation. *Wirel. Pers. Commun.* **2021**, *116*, 3261–3276. [CrossRef]
25. Parupalli, S.; Panyala, K. Performance Evaluation of Different PSK Schemes in an OFDM System Using a Real Time Image. *Wirel. Pers. Commun.* **2021**, *121*, 1391–1404. [CrossRef]
26. Hoydis, J.; Ten Brink, S.; Debbah, M. Massive MIMO: How many antennas do we need? In Proceedings of the 2011 49th Annual Allerton Conference on Communication, Control, and Computing (Allerton), Monticello, IL, USA, 28–30 September 2011; pp. 545–550.
27. Banelli, P.; Buzzi, S.; Colavolpe, G.; Modenini, A.; Rusek, F.; Ugolini, A. Modulation formats and waveforms for 5G networks: Who will be the heir of OFDM?: An overview of alternative modulation schemes for improved spectral efficiency. *IEEE Signal Processing Mag.* **2014**, *31*, 80–93. [CrossRef]
28. Zhang, Q.; Jin, S.; McKay, M.; Morales-Jimenez, D.; Zhu, H. Power allocation schemes for multicell massive MIMO systems. *IEEE Trans. Wirel. Commun.* **2015**, *14*, 5941–5955. [CrossRef]
29. Kaur, K.; Miglani, R.; Malhotra, J.S. Analysis of MIMO FSO over different Modulation Techniques. *Pertanika J. Sci. Technol.* **2017**, *25*, 905–9017.
30. Krishna, D.; Anuradha, M. Image Transmission through OFDM System under the Influence of AWGN Channel. *IOP Conf. Ser. Mater. Sci. Eng.* **2017**, *225*, 012217. [CrossRef]
31. Patel, J.; Seto, M. Live RF Image Transmission using OFDM with RPi and PlutoSDR. In Proceedings of the 2020 IEEE Canadian Conference on Electrical and Computer Engineering (CCECE), London, ON, Canada, 30 August–2 September 2020; pp. 1–5. [CrossRef]
32. Reddy, A.Y.; Reddy, B.L.; Sai, A.S.; Anuraj, K. MSE and BER Analysis of Text, Audio and Image Transmission Using ML Based OFDM. In Proceedings of the 2020 IEEE International Conference for Innovation in Technology (INOCON), Bangluru, India, 6–8 November 2020; pp. 1–3. [CrossRef]
33. Chandra, M.; Agarwal, D.; Bansal, A. Performance analysis of image transmission through Rayleigh channel. In Proceedings of the 2017 8th International Conference on Computing, Communication and Networking Technologies (ICCCNT), Delhi, India, 3–5 July 2017; pp. 1–5. [CrossRef]
34. Agarwal, A.; Kumar, B.S.; Agarwal, K. BER Performance Analysis of Image Transmission Using OFDM Technique in Different Channel Conditions Using Various Modulation Techniques. In *Computational Intelligence in Data Mining*; Behera, H.S., Nayak, J., Naik, B., Abraham, A., Eds.; Springer: Singapore, 2019; pp. 1–8. [CrossRef]

35. Esmaiel, H.; Jiang, D. Progressive ZP-OFDM for Image Transmission Over Underwater Time-Dispersive Fading Channels. In Proceedings of the 2018 International Conference on Computing, Electronics Communications Engineering (iCCECE), Southend, UK, 16–17 August 2018; pp. 226–229. [CrossRef]
36. Mannan, A.; Habib, A. Adaptive processing of image using DWT and FFT OFDM in AWGN and Rayleigh channel. In Proceedings of the 2017 International Conference on Communication, Computing and Digital Systems (C-CODE), Islamabad, Pakistan, 8–9 March 2017; pp. 346–350. [CrossRef]
37. Rajesh, V.; Rajak, A.R.A. Channel estimation for image restoration using OFDM with various digital modulation schemes. *J. Phys. Conf. Ser.* **2020**. *1706*, 012076. [CrossRef]
38. Helen, C.N.; Judson, D. Image Transmission in Multi Carrier CDMA System with Different Equalization Techniques. In Proceedings of the 2019 International Conference on Recent Advances in Energy-efficient Computing and Communication (ICRAECC), Nagercoil, India, 7–8 March 2019; pp. 1–5. [CrossRef]
39. Sarala, B.; Zaheer Ahamed, M.; Sree Hari, S.; Bhagya sree, V. Voice and Image BER Analysis of the OFDM System with MECCT and MLNST Companding Techniques Over Mobile Radio Channels. In *Innovations in Electrical and Electronics Engineering*; Saini, H.S., Srinivas, T., Vinod Kumar, D.M., Chandragupta Mauryan, K.S., Eds.; Springer: Singapore, 2020; pp. 777–785. [CrossRef]
40. Amhoud, E.M.; Othman, G.R.B.; Bigot, L.; Song, M.; Andresen, E.R.; Labroille, G.; Bigot-Astruc, M.; Jaouën, Y. Experimental demonstration of space-time coding for MDL mitigation in few-mode fiber transmission systems. In Proceedings of the 2017 European Conference on Optical Communication (ECOC), Gothenburg, Sweden, 17–21 September 2017; pp. 1–3.
41. Ghanim, Z.N.; Omran, B.M. OFDM PAPR reduction for image transmission using improved tone reservation. *Int. J. Electr. Comput. Eng. (2088-8708)* **2021**, *11*, 416–423. [CrossRef]
42. Judson, D.; Devi, T.A.; Helen, C.N. Performance Analysis of Image Transmission with Different Transforms in MC-CDMA. In Proceedings of the 2019 International Conference on Recent Advances in Energy-Efficient Computing and Communication (ICRAECC), Nagercoil, India, 7–8 March 2019; pp. 1–5. [CrossRef]
43. Wang, Z.P.; Ye, Z.Y.; Wang, X.M.; Zhai, Z.N. Image transmission in an OFDM VLC system using symbol scrambling and chaotic Walsh-Hadamard precoding. *Optoelectron. Lett.* **2019**, *15*, 284–287. [CrossRef]
44. Sakthivel, S.; Pradeep, N. reciprocal data map coding scheme for image transmission in MIMO-OFDM systems. *Wirel. Pers. Commun.* **2018**, *103*, 3145–3161. [CrossRef]
45. Amhoud, E.M.; Othman, G.R.B.; Jaouën, Y. Concatenation of space-time coding and FEC for few-mode fiber systems. *IEEE Photonics Technol. Lett.* **2017**, *29*, 603–606. [CrossRef]
46. Sohtsinda, H.; Perrine, C.; Bachir, S.; Duvanaud, C.; Chatellier, C. Amplifier-Aware Content-Based Precoder Design for Hierarchical Image Transmission over a Realistic MIMO-OFDM Channel. *J. Circuits Syst. Comput.* **2019**, *28*, 1950209. [CrossRef]
47. Youssef, M.; Emam, A.E.; Abd Elghany, M. Image multiplexing using residue number system coding over MIMO-OFDM communication system. *Int. J. Electr. Comput. Eng.* **2019**, *9*, 4815–4825. [CrossRef]
48. Kansal, L.; Gaba, G.S.; Chilamkurti, N.; Kim, B.G. Efficient and Robust Image Communication Techniques for 5G Applications in Smart Cities. *Energies* **2021**, *14*, 3986. [CrossRef]
49. Miglani, R.; Malhotra, J.S. Investigation on R–S coded coherent OFDM free space optical (CO-OFDM-FSO) communication link over gamma–gamma channel. *Wirel. Pers. Commun.* **2019**, *109*, 415–435. [CrossRef]
50. Weinstein, S.; Ebert, P. Data transmission by frequency-division multiplexing using the discrete Fourier transform. *IEEE Trans. Commun. Technol.* **1971**, *19*, 628–634. [CrossRef]
51. Stone, H.S. R66-50 an algorithm for the machine calculation of complex fourier series. *IEEE Trans. Electron. Comput.* **1966**, *15*, 680–681. [CrossRef]
52. Amhoud, E.M.; Chafii, M.; Nimr, A.; Fettweis, G. OFDM with Index Modulation in Orbital Angular Momentum Multiplexed Free Space Optical Links. In Proceedings of the 2021 IEEE 93rd Vehicular Technology Conference (VTC2021-Spring), Helsinki, Finland, 25–28 April 2021; pp. 1–5.
53. Asif, R.; Abd-Alhameed, R.A.; Oanoh, O.; Dama, Y.; Migdadi, H.; Noars, J.; Hussaini, A.S.; Rodriguez, J. Performance comparison between DWT-OFDM and FFT-OFDM using time domain zero forcing equalization. In Proceedings of the 2012 International Conference on Telecommunications and Multimedia (TEMU), Heraklion, Greece, 30 July–1 August 2012; pp. 175–179. [CrossRef]
54. Ozaktas, H.M.; Arikan, O.; Kutay, M.A.; Bozdagt, G. Digital computation of the fractional Fourier transform. *IEEE Trans. Signal Process.* **1996**, *44*, 2141–2150. [CrossRef]
55. Taherpour, A.; Andargoli, S.M.; Ghods, V. Joint power allocation and user assignment for licensed/unlicensed band users in massive MIMO cellular systems. *Phys. Commun.* **2022**, *52*, 101590. [CrossRef]
56. Mokhtari, Z.; Sabbaghian, M.; Dinis, R. Massive MIMO downlink based on single carrier frequency domain processing. *IEEE Trans. Commun.* **2016**, *66*, 1164–1175. [CrossRef]